Effects of magnetic ions on optical properties: the case of (Ga, Fe)N

2008 J. Phys.: Condens. Matter 20 454222

(http://iopscience.iop.org/0953-8984/20/45/454222)

J. Phys.: Condens. Matter **20** (2008) 454222 (6pp) doi:10.1088/0953-8984/20/45/454222

Effects of magnetic ions on optical properties: the case of (Ga, Fe)N

M Wegscheider[1], Tian Li[1], A Navarro-Quezada[1], B Faina[1], A Bonanni[1], W Pacuski[2], R Jakieła[3] and T Dietl[3,4]

[1] Institute for Semiconductor and Solid State Physics, Johannes Kepler University, Altenbergerstrasse 69, A-4040, Linz, Austria
[2] Institute of Experimental Physics, University of Warsaw, Hoża 69, PL-00-681 Warszawa, Poland
[3] Institute of Physics, Polish Academy of Sciences, aleja Lotników 32/46, PL 02-668 Warszawa, Poland
[4] Institute of Theoretical Physics, University of Warsaw, ulica Hoża 69, PL-00-681 Warszawa, Poland

E-mail: alberta.bonanni@jku.at and dietl@ifpan.edu.pl

Received 26 May 2008, in final form 10 July 2008
Published 23 October 2008
Online at stacks.iop.org/JPhysCM/20/454222

Abstract
Because of strong exchange interactions between localized spins and effective mass carriers, transition metal impurities in semiconductors lead to giant magneto-optical effects. Furthermore, band-gap levels derived from open d shells of magnetic impurities act as efficient recombination centers for photo-carriers. This paper reviews studies of excitonic magneto-reflectivity performed on (Ga, Fe)N epilayers, and shows how hybridization between d levels and band states, particularly strong in nitrides and oxides, renormalizes the exchange splitting of the valence band states in these systems. Photoluminescence measurements on the same structures demonstrate an increase of infrared Fe-related emission at the expense of ultraviolet near band-gap luminescence. This sensitivity of luminescence to the presence of Fe impurities is exploited to monitor the aggregation of Fe_xN nanocrystals that account for the room temperature ferromagnetism of (Ga, Fe)N, but do not act as inhibitors of excitonic luminescence.

(Some figures in this article are in colour only in the electronic version)

1. Introduction

There is an increasing awareness that further progress in the development of functional material systems based on diluted magnetic semiconductors (DMSs) requires the ability to control the incorporation and distribution of magnetic ions by growth conditions and co-doping with shallow impurities [1, 2] as well as an understanding of the complex interplay between carrier-mediated exchange and carrier localization [3]. In this paper we discuss the results of magneto-reflectivity and photoluminescence studies carried out on (Ga, Fe)N epilayers, which (i) show how strong coupling between magnetic ions and hole states *reduces* the valence band exchange splitting and (ii) demonstrate a dramatic effect of the growth rate on the nano-assembly of ferromagnetic nanocrystals.

2. sp–d(f) exchange interactions in DMSs

It is well known that giant magneto-optical and magneto-transport phenomena as well as carrier-mediated ferromagnetic interactions specific to DMSs result from exchange couplings between band carriers and open d or f shells of transition metal (TM) or rare earth (RE) ions, respectively. Studies of magneto-optical properties have been particularly extensive in the case of Mn-based II–VI DMSs [4–7] as well as in Mn- and Eu-based IV–VI DMSs [8], where the sp–d(f) exchange contributes to or even dominates the spin-splitting of band states. Importantly, as shown first by Günther Bauer and co-workers, the photo-carriers not only experience the molecular field produced by magnetic impurities but also affect their spin polarization [9, 10].

In II–VI and IV–VI DMS systems, the divalent Mn and Eu assume the high spin state, d^5, $S = 5/2$ and f^7, $S = 7/2$, respectively and also act as isoelectronic impurities that neither donate nor trap carriers. The corresponding temperature- and magnetic-field-dependent magnetization is described by a modified Brillouin function [5],

$$M(T, H) = x_{\text{eff}} N_0 g \mu_B S B_S(T + T_{\text{AF}}, H), \qquad (1)$$

where the influence of intrinsic antiferromagnetic interactions is included into two phenomenological parameters: a reduced concentration of magnetic ions, $x_{\text{eff}} N_0$, which accounts for the presence of magnetically neutral nearest-neighbor singlet pairs, and an enhanced temperature $T + T_{\text{AF}}$, describing the molecular field produced by next-nearest-neighbors.

The presence of randomly distributed magnetic impurities can then be incorporated into the effective mass theory within the time-honored virtual-crystal (VCA) and molecular-field (MFA) approximations, that is by adding to the kp Hamiltonian a Zeeman-like term, $I\vec{s}\vec{M}/g\mu_B$. Here I is an exchange operator, whose matrix elements between periodic parts of band-edge wavefunctions constitute exchange integrals. Their values have been determined quite accurately for a number of DMSs by comparing experimental and theoretical spin-splittings as a function of temperature and magnetic field [8, 11]. Rather generally, there are two mechanisms controlling the magnitude of these integrals [11–15], namely the intra-atomic potential exchange and the spin-dependent hybridization between band and localized states, known as the kinetic exchange.

3. Break-down of VCA and MFA in DMSs

There is a growing amount of evidence that the above clear-cut picture requires serious modifications in a variety of cases. In particular, difficulties in the description of magneto-optical data as a function of temperature and Mn concentration x by employing one set of the exchange integrals have been persistently reported for narrow-gap II–VI [16] and IV–VI [17] DMSs. While it cannot be ruled out that these interpretation problems reflect inaccuracies of a multi-parameter fitting procedure inherent in narrow-gap semiconductors, it has been pointed out that a large relativistic downwards shift of the s states in heavy Hg and Pb atoms, compared with the case of lighter transition metal ions, may render the VCA invalid in narrow-gap DMSs [15].

However, the case of wide band-gap II–VI DMSs is particularly striking. While the VCA and MFA describe very properly the giant exciton splittings in tellurides [5], their accuracy has been called into question in the case of $Cd_{1-x}Mn_xS$ [18]. In this system, unexpected dependences of the band-gap and of the apparent p–d exchange integral $\beta^{(\text{app})}$ on x have been explained by circumventing VCA and MFA either by employing a non-perturbative Wigner–Seitz-type model [18] or generalizing the alloy theory to DMSs [19]. In II–VI oxides, a small bond length and, thus, strong p–d hybridization, should result in a large value of $N_0|\beta|$, a prediction supported by photoemission experiments [20]. Surprisingly, however, some of the present authors found abnormally small exciton splittings in (Zn, Co)O [21] and (Zn, Mn)O [22]. Prompted by these observation, a theory has been put forward [23] which shows that the strong p–d coupling makes the *apparent* exchange energy $N_0\beta^{(\text{app})}$ describing the valence band splitting small and of opposite sign. Importantly, the system bears some similarity with semiconductor alloys such as (Ga, N)As, so that experimental and theoretical studies of the valence band exchange splitting in the strong coupling limit may significantly improve our understanding of these alloys [24].

4. Excitonic magneto-reflectivity in (Ga, Fe)N

To check the above model, magnetization and magneto-reflectivity in the free exciton region of (Ga, Fe)N epilayers have been studied [25]. Since in GaN—in contrast to ZnO—the actual ordering of valence subbands is settled, the sign of $N_0\beta^{(\text{app})}$ can be unambiguously determined from polarization-resolved magneto-optical spectra. Furthermore, unlike Mn, Fe in GaN is an isoelectronic impurity with the simple d^5 configuration [26, 27], allowing a straightforward interpretation of the data.

The 0.7 μm thick layers of $Ga_{1-x}Fe_xN$ were grown by metalorganic vapor phase epitaxy (MOVPE) on [0001] sapphire substrates with a 1 μm thick, wide band-gap (Ga, Al)N buffer layer, which is transparent in the free exciton region of $Ga_{1-x}Fe_xN$. The Fe content was kept well below 0.4%, the solubility limit of Fe in GaN under our growth conditions. According to detailed luminescence, electron paramagnetic resonance and magnetic susceptibility studies [26], in this range the Fe ions mostly assume the expected Fe^{3+} charge state (d^5 configuration).

Magneto-reflectivity spectra were collected in the Faraday configuration (propagation of light and magnetic field along the normal to the sample, which is the c-axis of the wurtzite structure), and with the light helicity $\sigma^{\pm}$ defined with respect to the magnetic field direction. On these high quality layers, either two or the three free excitons of GaN, A, B, C, are resolved, and their Zeeman shifts are visible in the spectra reported in figures 1(a), (c). In σ^- polarization, the A–B splitting increases and the B–C splitting decreases with the field. Opposite shifts are observed in σ^+. These shifts are entirely different from those observed in pure GaN [28] and are related to the magnetization, implying that the Fe ions create a giant Zeeman effect in (Ga, Fe)N. However, at given x, the shift observed for exciton A is opposite in sign and significantly smaller than in other wurtzite DMSs with d^5 ions like (Cd, Mn)Se [29].

The methodology employed to extract the values of the apparent p–d exchange energy $N_0\beta^{(\text{app})}$ for the valence band and the apparent s–d exchange energy $N_0\alpha^{(\text{app})}$ for the conduction band from the data involved two major steps [25]. First, the reflection coefficients as a function of the photon energy were calculated by using a polariton model incorporating the ground states of excitons A and B but also exciton C, excited states of excitons, and the continuum. In the second step, the field dependence of the exciton energies was calculated including the trigonal component of both crystal

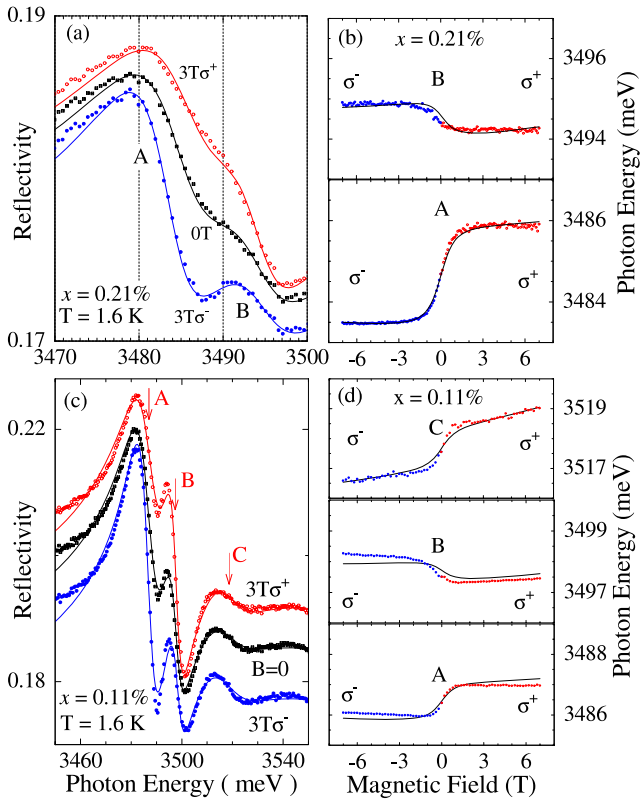

Figure 1. Reflectivity of $Ga_{1-x}Fe_xN$ in Faraday configuration at 1.6 K for $x = 0.21\%$ (a) and 0.11% (c) where particularly well-resolved excitons A, B and C are visible in σ^- polarization. (b), (d) Field-induced exciton shifts of the excitons determined from the polariton model (points) compared to the expectations of the exciton model (solid lines). The determined values of the exchange parameters are $N_0\beta^{(\mathrm{app})} = +0.5 \pm 0.2$ eV and $N_0\alpha^{(\mathrm{app})} = +0.1 \pm 0.2$ eV (after [25]).

field and biaxial strain as well as the anisotropic spin–orbit interaction and the electron–hole interaction within the exciton. Effects linear in the magnetic field are taken into account within the relevant kp model and allow for a diamagnetic shift. The standard form of the s, p–d Hamiltonian was used [7, 11, 29], treating $\alpha^{(\mathrm{app})}$ and $\beta^{(\mathrm{app})}$ as fitting parameters.

The fitting procedure, whose results are presented in figures 1(b), (d), yielded $N_0\beta^{(\mathrm{app})} = +0.5 \pm 0.2$ eV and $N_0\alpha^{(\mathrm{app})} = +0.1 \pm 0.2$ eV. We note that this evaluation of $N_0\alpha^{(\mathrm{app})}$ includes within the experimental error the values of $N_0\alpha = 0.25 \pm 0.06$ eV found in early studies of Mn-based II–VI DMSs [11]. We have no reason to question here the applicability of the standard description of the conduction band in (Ga, Fe)N—contrary to (Ga, Mn)As and (Ga, Mn)N, for which the magnitudes of $N_0\alpha^{(\mathrm{app})}$ were found to be reduced under some experimental conditions [30]. For the expected d level arrangement, both the ferromagnetic sign and the small magnitude of the apparent p–d exchange energy are surprising. Indeed, in GaN the Fe d^5/d^6 acceptor-like level resides less than 3 eV above the top of the valence band [27]. This state, $e_g\downarrow$, and also the higher lying $t_2\downarrow$ level that can hybridize with the valence band states, remain unoccupied in intrinsic (Ga, Fe)N. At the same time, no donor-like d^5/d^4 state has been found within the GaN gap. This could be expected, as in the TM series a particularly large correlation energy U separates the d^5 and d^6 shells. Hence, the occupied Fe $t_2\uparrow$ levels reside within the valence band. According to the Schrieffer–Wolf theory, in such a case the p–d exchange coupling is antiferromagnetic: this was confirmed by magneto-optical studies of tellurides and selenides containing either Mn or Fe, including studies carried out in our labs, which lead systematically to $N_0\beta = -1.4 \pm 0.5$ eV [11].

However, it has been recently remarked [23] that for an appropriately strong TM potential like the one expected for oxides and nitrides, the TM ion can bind a hole—a trend which had already been suggested by strong deviations from the VCA in (Cd, Mn)S [18] and by the results of a numerical diagonalization of a model DMS Hamiltonian [31]. A summation of infinite series of relevant self-energy diagrams demonstrates that the spin-splitting of extended states involved in the optical transitions remains proportional to the magnetization, but the apparent exchange energy becomes significantly renormalized [23]. For the expected coupling strength, the theory predicts $-1 < \beta^{(\mathrm{app})}/\beta < 0$, as observed for (Ga, Fe)N.

5. Strong coupling and ferromagnetism of wide band-gap DMSs

The magneto-optical results discussed above revealed the presence of strong coupling between holes and localized spins in nitrides and oxides. This means, in particular, that TM ions bind holes in these systems, precluding the occurrence of carrier-mediated ferromagnetism in p-type materials. However, at high hole densities, an insulator-to-metal transition is expected. In the metallic phase, the many-body screening of local potentials annihilates the bound states. Large spin-splitting and robust ferromagnetism are anticipated in this regime [23], an expectation waiting for an experimental proof.

However, it is well known that despite the absence of holes a number of wide-band-gap semiconductors and oxides shows ferromagnetic-like signatures persisting up to above room temperature [2, 32, 33]. According to the present insight, this ferromagnetism is to be linked to a self-organized aggregation of magnetic nanocrystals embedded in a paramagnetic host [23, 26]. Importantly, as we show below, the aggregation process in the case of (Ga, Fe)N, along with element-sensitive microscopy and synchrotron-radiation diffraction [34], can be probed by photoluminescence.

6. Effect of Fe aggregation on the photoluminescence

We recently demonstrated that the aggregation of magnetic ions in a GaN matrix can be controlled by varying the growth rate and co-doping with Si and Mg [34]. In particular, the increasing growth rate hinders the aggregation of Fe ions and, thus, enlarges the concentration of the Fe ions occupying randomly substitutional Ga sites in the GaN matrix [34].

A series of (Ga, Fe)N layers has been grown by MOVPE according to the protocols we already reported [26]. The samples have been fabricated at a constant growth temperature

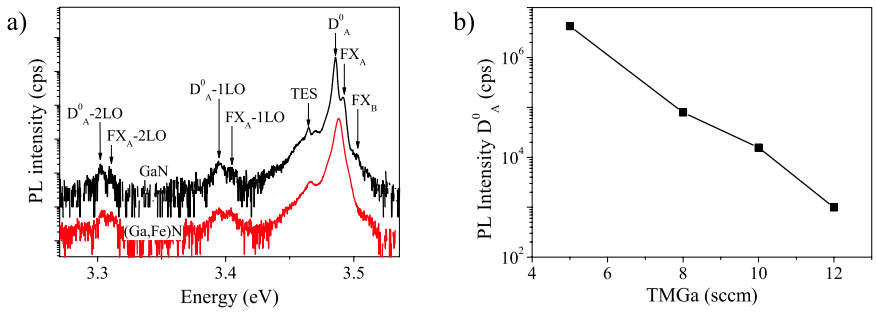

Figure 2. (a) Excitonic luminescence at 10 K for a nominally undoped GaN sample (topmost curve) and for a (Ga, Fe)N sample (lower curve) with the lowest growth rate (corresponding to TMGa = 5 sccm). (b) Maximum peak intensity of donor-bound exciton emission versus TMGa flow-rate (growth rate).

of 850 °C and the growth rate—regulated by the Ga-precursor flow-rate (TMGa)—was changed for each sample and scales about linearly, attaining 0.3 nm s^{-1} for 12 sccm of TMGa flow. The layers have been studied by means of photoluminescence (PL), transmission electron microscopy (TEM) and secondary ion mass spectroscopy (SIMS). The PL measurements are performed in the near infrared (IR) and ultraviolet (UV) range by using a HeCd laser with an output power of 40 mW, a monochromator with focal length 550 mm and a nitrogen cooled 1024 × 512 pixel CCD camera. The samples are situated in a He-flow cryostat which allows measurements down to 5 K and where the incident excitation power is approximately 1.2 W cm^{-2}. TEM measurements were carried out in a JEOL 2011 fast TEM microscope operating at 200 kV.

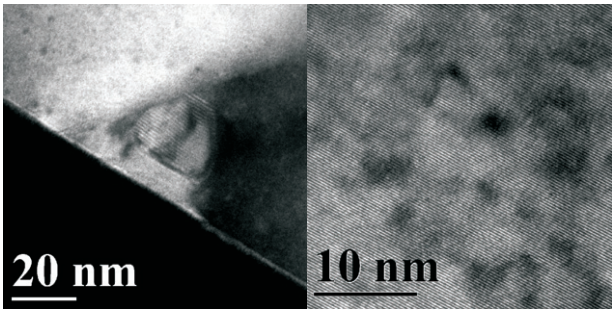

Figure 3. TEM micrographs reveal the presence of nanocrystals (left panel) in samples deposited at the lowest growth rate (TMGa = 5 sccm) and spinodal decomposition (right panel) in the structures fabricated with a TMGa flow-rate of 8 sccm.

6.1. Excitonic recombination versus spinodal decomposition

Low temperature PL measurements on nominally undoped GaN reveal a typical excitonic emission dominated by an exciton bound to shallow donors (D^0_A) with a maximum at 3.486 eV, as shown in figure 2(a). Additionally, this near-band-edge emission consists of the free excitons FX_A and FX_B located at the high energy tail of the spectrum, as well as a two-electron satellite (TES) and the LO phonon replica D^0_A-LO and FX_A-LO at energies reduced by 91 meV [35, 36]. Fe as an impurity in III–V semiconductors is known as a lifetime killer of the excitonic recombination [37]; nevertheless, in the samples deposited at the lowest growth rates we can measure the specific near-band-edge emission, as shown in figure 2(b). Temperature-dependent measurements [38] and comparison with the case of nominally undoped layers, show that the excitonic emissions measured on the (Ga, Fe)N samples are basically the same as those from pure GaN.

In order to correlate these findings with the actual structure and Fe incorporation into the layers, we performed (high resolution) TEM experiments that reveal either the formation of Fe-rich secondary phases of Fe_3N or spinodal decomposition into regions respectively rich and poor in magnetic ions [34].

In the sample fabricated at the lowest growth rate for which the highest intensity of excitonic luminescence is measured, the presence of nanocrystals is confirmed by the TEM image reported in figure 3 (left panel). Additionally, in such samples a gradient in the Fe distribution has been noted, so that the large magnitude of the PL intensity may originate from regions depleted of Fe. In layers deposited at intermediate growth rates the excitonic recombination starts to quench and the TEM analysis reveals the presence of regions of spinodal decomposition like the one reported in figure 3 (right panel). In samples produced at the highest growth rates the excitonic luminescence intensity is actually reduced by about three orders of magnitude and TEM images uncover an intact crystal structure where the Fe ions are homogeneously incorporated mostly in substitutional sites.

6.2. Effect of growth rate upon Fe^{3+}- and defect-related recombination

The infrared spectra reported in figure 4 were acquired at 5 K and show the emission related to the $^4T_1(G)$–$^6A_1(S)$ intra-ionic transition of Fe in its 3+ (d^5) configuration [39] with a maximum at 1.299 eV, two weakly excited states between 1.300 and 1.302 eV and with a characteristic vibrational sideband. In the inset to figure 4, the integrated intensities of PL related to these intra-ionic Fe^{3+} transitions are seen to decrease with the growth rate. Two effects may reduce the emission intensity: (i) the incorporation of Fe ions in the nanocrystals lowering the concentration of Fe^{3+} diluted into the matrix and contributing to the intra-ionic emission and (ii) competing recombination processes where photo-carriers choose different radiative and non-radiative channels.

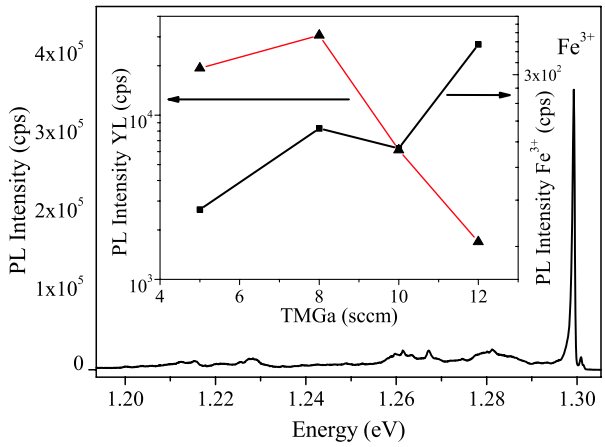

Figure 4. Fe^{3+}-related intra-ionic $^4T_1(G)$–$^6A_1(S)$ emission at 5 K. Inset: integrated PL intensities of the Fe^{3+} and yellow defect band emission as a function of Ga flow-rate.

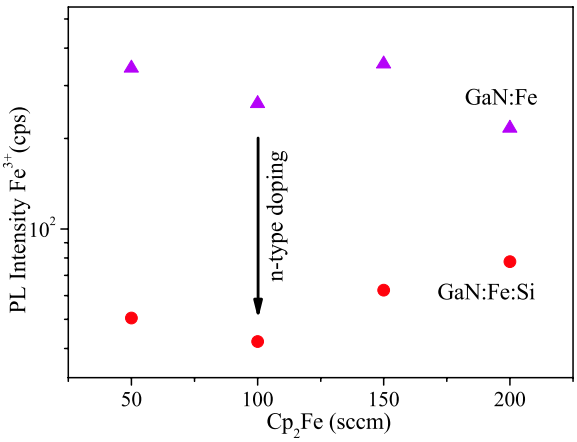

Figure 5. Integrated intensity of the Fe^{3+}-related intra-ionic $^4T_1(G)$–$^6A_1(S)$ transition at 5 K as a function of the Fe-precursor flow-rate. The quenching of the intensity upon co-doping with Si is evident.

One of the competing radiation channels is exciton luminescence appearing when the concentration of randomly distributed Fe^{3+} decreases, as discussed in the previous section. As a fingerprint of another competing radiative recombination center, the authors of [40] proposed the yellow defect (YL) band. The origin of this luminescence is still not clarified, but it is likely that Ga vacancies, either single or related to impurities, like defect complexes with shallow donors or hydrogen, are involved [41]. In agreement with this model, the YL intensity is found to be reduced by increasing the Ga-precursor flow-rate (thus by changing the Ga/N ratio during growth) as well as by increasing the Fe content known to compensate the carrier background with a consequent increment of the formation energy of Ga vacancies [42]. Indeed our PL measurements reveal a decrease in the integrated intensity of the YL band with the TMGa flow-rate, as evidenced in figure 4, with a raising of the Fe^{3+}-related emission intensity as a counter-effect. The intensity of the YL (with a maximum at 2.200 eV) and of the Fe^{3+}-related emission have been integrated and reported in the inset to figure 4. Threading dislocations, mainly due to the considerable strain induced by the mismatch between the sapphire substrate and the GaN overlayer, have been proposed as further recombination centers [43], but the incorporation of Fe is found not to affect the density of dislocations in our layers [44].

It has recently been demonstrated that co-doping of (Ga, Fe)N with Si or Mg hampers the aggregation of magnetic ions [34]. The effect has been attributed to the dependence of attractive forces between magnetic ions on their valence, i.e. the charge state, which can be altered by co-doping. This novel mechanism of control over nano-assembly of nanostructures will be functional, provided that the relevant magnetic ion gives rise to band-gap levels. It is, therefore, interesting to monitor how the co-doping affects the intra-ion luminescence specific to Fe in the 3+ charge state. Actually, according to our preliminary findings [26], the Si co-doping reduces while Mg co-doping enhances the intensity of this luminescence.

Results of additional studies are presented in figure 5. This shows that indeed the Fe^{3+} ions are converted to the Fe^{2+} configuration in the presence of a sufficient number of electrically active donors. However, competition with the YL-related radiative channel—showing an increase in intensity due to a decrease in the formation energy of Ga vacancies upon a shift of the Fermi level—may also be involved.

In the case of co-doping with Mg acceptors, in contrast, the Fe^{3+}-related PL intensity is found to increase [26], the effect being assigned to the capture by Mg acceptors of electrons supplied by residual donors, which results in an increase in the Fe^{3+} concentration. Furthermore, referring to section 4, we note that the potential introduced by the Fe ion is sufficiently strong in GaN to bind a hole in a charge transfer state, $Fe^{3+} + h$. Such trapping may results in an admixture of the p-type wavefunction into the Fe d wavefunctions, which may enhance the probability of intra-ion transitions that are parity forbidden in the absence of a hole. It is interesting to note that a many-body enhancement of intra-ionic $^4T_1(G)$–$^6A_1(S)$ transitions upon p-type doping was noted by some of us in the case of (Zn, Mn)Te:N [45], where Mn^{2+} ions are in the same d^5, $S = 5/2$ configuration as Fe^{3+} ions in GaN. The studies of these effects are under way, also employing delta doping with Mg and Fe.

7. Summary

Studies of excitonic magneto-reflectivity and luminescence performed on (Ga, Fe)N epilayers have provided important information on the non-standard renormalization of extended states by transition metal impurities in wide-band-gap semiconductors and demonstrated the sensitivity of the optical emission to the distribution of magnetic ions. This distribution has been found to exert a strong influence on intra-ion emission as well as on defect-related radiative recombination. In general terms, the results presented here and previously for (Ga, Fe)N [26, 34], as well as parallel works on oxides carried out by other groups [46], demonstrate clearly that a further

progress in the understanding of the physics of DMSs and oxides requires comprehensive studies as a function of growth conditions and co-doping, employing a pallet of state-of-the art characterization methods.

Acknowledgments

We thank Günther Bauer for many valuable discussions concerning the work described in this paper. Two of us (AB and TD) would like to express our gratitude for his continuous encouragement and guidance over many recent years. This work has been supported by the Austrian Fonds zur Förderung der wissenschaftlichen Forschung-FWF (projects P17169, P20065 and N107-NAN), and by the European Community (projects NANOSPIN, FP6-2002-IST-015728 and SPINTRA, ERAS-CT-2003-980409).

References

[1] Dietl T and Ohno H 2006 *Mater. Today* **9** 18
[2] Dietl T 2008 *J. Appl. Phys.* **103** 07D111
[3] Dietl T 2008 *J. Phys. Soc. Japan* **77** 031005
[4] Bastard G, Rigaux C, Guldner Y, Mycielski J and Mycielski A 1978 *J. Physique* **39** 87
[5] Gaj J A, Planel R and Fishman G 1979 *Solid State Commun.* **29** 435
[6] Bauer G, Kossut J, Faymonville R and Dornhaus R 1985 *Phys. Rev.* B **31** 2040
[7] Furdyna J K and Kossut J 1988 Diluted magnetic semiconductors *Semiconductor and Semimetals* vol 25, ed S Chikazumi and N Miura (New York: Academic)
[8] Bauer G, Pascher W and Zawadzki W 1992 *Semicond. Sci. Technol.* **7** 703
[9] Krenn H, Zawadzki W and Bauer G 1985 *Phys. Rev. Lett.* **55** 1510
[10] Krenn H, Kaltenegger K, Dietl T, Spałek J and Bauer G 1989 *Phys. Rev.* B **39** 10918
[11] Kacman P 2001 *Semicond. Sci. Technol.* **16** R25
[12] Dietl T 1981 Semimagnetic semiconductors in high magnetic fields *Physics in High Magnetic Fields* ed S Chikazumi and N Miura (Berlin: Springer) p 344
[13] Bhattacharjee A K, Fishman G and Coqblin B 1983 *Physica* B+C **117** 449
[14] Larson B E, Hassand K C, Ehrenreich H and Carlsson A E 1988 *Phys. Rev.* B **37** 4137
[15] Dietl T, Śliwa C C, Bauer G and Pascher H 1994 *Phys. Rev.* B **49** 2230
[16] Dobrowolska M, Dobrowolski W, Otto M, Dietl T and Galazka R R 1980 *J. Phys. Soc. Japan* **49** 815
[17] Pascher H, Röthlein P, Bauer G and von Ortenberg M 1989 *Phys. Rev.* B **40** 10469
[18] Benoit à la Guillaume C, Scalbert D and Dietl T 1992 *Phys. Rev.* B **46** 9853(R)
[19] Tworzydlo A 1995 *Acta Phys. Pol.* A **88** 655
[20] Mizokawa T, Nambu T, Fujimori A, Fukumura T and Kawasaki M 2005 *Phys. Rev.* B **65** 085209
[21] Pacuski W, Ferrand D, Cibert J, Deparis C, Gaj J A, Kossacki P and Morhain C 2006 *Phys. Rev.* B **73** 035214
[22] Przeździecka E, Kamińska E, Kiecana M, Sawicki M, Kłopotowski Ł, Pacuski W and Kossut J 2006 *Solid State Commun.* **139** 541
[23] Dietl T 2008 *Phys. Rev.* B **77** 085208
[24] Wu J, Shan W and Walukiewicz W 2002 *Semicond. Sci. Technol.* **17** 860
[25] Pacuski W *et al* 2008 *Phys. Rev. Lett.* **100** 037204
[26] Bonanni A *et al* 2007 *Phys. Rev.* B **75** 125210
[27] Malguth E, Hoffmann A and Phillips M R 2008 *Phys. Status Solidi* b **245** 455
[28] Stępniewski R, Potemski M, Wysmołek A, Pakuła K, Baranowski J M, Łusakowski J, Grzegory I, Porowski S, Martinez G and Wyder P 1999 *Phys. Rev.* B **60** 4438
[29] Arciszewska M and Nawrocki M 1986 *J. Phys. Chem. Solids* **47** 309
[30] Śliwa C and Dietl T 2008 *Preprint* 0707.3542 [cond-mat.mtrl-sci]
[31] Bouzerar R, Bouzerar G and Zimai T 2007 *Europhys. Lett.* **78** 67003
[32] Liu C, Yun F and Morkoç H 2005 *J. Mater. Sci.* **16** 555
[33] Bonanni A 2007 *Semicond. Sci. Technol.* **22** R41
[34] Bonanni A *et al* 2008 *Preprint* 0804.3324v1 [cond-mat.mtrl-sci]
[35] Davydov V Yu, Kitaev Yu E, Goncharuk I N, Smirnov A N, Graul J, Semchinova O, Uffmann D, Smirnov M B, Mirgorodsky A P and Evarestov R A 1998 *Phys. Rev.* B **58** 12899
[36] Monemar B 2001 *J. Phys.: Condens. Matter* **13** 7011
[37] Bishop S 1992 *Deep Centers in Semiconductors* (New York: Gordon and Breach) p 541
[38] Wegscheider M, Simbrunner C, Przybylinska H, Kiecana M, Sawicki M, Navarro-Quezada A, Sitter H, Jantsch W, Dietl T and Bonanni A 2006 *Phys. Status Solidi* a **204** 86
[39] Malguth E, Hoffmann A, Gehlhoff W, Gelhausen O, Phillips M R and Xu X 2006 *Phys. Rev.* B **74** 165202
[40] Hoffmann A *et al* 1997 *Solid State Electron.* **41** 275
[41] Reshchikov M A and Korotkov R Y 2001 *Phys. Rev.* B **64** 115205
[42] Reshchikov M A and Morkoc H 2005 *J. Appl. Phys.* **97** 061301
[43] You J H and Johnson H T 2007 *Phys. Rev.* B **76** 115336
[44] Li T 2008 unpublished
[45] Bonanni A, Hingerl K, Hilber W, Stifter D and Sitter H 2000 *J. Cryst. Growth* **214/215** 163
[46] Ney A, Ollefs K, Ye S, Kammermeier T, Ney V, Kaspar T C, Chambers S A, Wilhelm F and Rogalev A 2008 *Phys. Rev. Lett.* **100** 157201